materials

MDPI

Article

Nonlinear Magnetoelectric Response of $Fe_{73.5}Cu_1Nb_3Si_{13.5}B_9$/Piezofiber Composite for a Pulsed Magnetic Field Sensor

Caijiang Lu [1,*], Hai Zhou [1], Aichao Yang [2], Zhengyu Ou [1], Feihu Yu [1] and Hongli Gao [1]

[1] Department of Electromechanical Measuring and Controlling, School of Mechanical Engineering, Southwest Jiaotong University, Chengdu 610031, China
[2] Jiangxi Electric Power Research Institute, Nanchang 330096, China
* Correspondence: lucaijiang@swjtu.edu.cn or lucjpaper@163.com

Received: 25 June 2019; Accepted: 3 September 2019; Published: 5 September 2019

Abstract: In this paper, we report the nonlinear magnetoelectric response in a homogenous magnetostrictive/piezoelectric laminate material. The proposed magnetoelectric stack $Fe_{73.5}Cu_1Nb_3Si_{13.5}B_9$/piezofiber is made up of high-permeability magnetostrictive $Fe_{73.5}Cu_1Nb_3Si_{13.5}B_9$ foils and a piezoelectric Pb(Zr, Ti)O_3 fiber composite. The time dependence of magnetoelectric interactions in the $Fe_{73.5}Cu_1Nb_3Si_{13.5}B_9$/piezofiber structure driven by pulsed magnetic field was investigated in detail. The experimental results show that the magnetoelectric effect is strongly dependent on the external bias magnetic and pulsed magnetic field parameters. To detect the amplitude of a pulsed magnetic field, the output sensitivity reaches 17 mV/Oe, which is excited by a 100 μs width field. In addition, to measure the pulsed width, the output sensitivity reaches 5.4 mV/μs in the range of 0–300 μs. The results show that the proposed $Fe_{73.5}Cu_1Nb_3Si_{13.5}B_9$/piezofiber sensor is ideally suited for pulsed magnetic field measurement.

Keywords: magnetoelectric response; pulsed magnetic field sensor; piezofiber; composite

1. Introduction

Magnetic field sensors are widely used in various fields, for example, in the industry, agriculture, medicine, aerospace, marine, exploration, and drilling. In recent years, the magnetoelectric (ME) composites with a product property of magnetostrictive and piezoelectric phases have been of great importance for the realization of a magnetic sensor [1–3]. In the ME effect, an electric field is induced under the application of a magnetic field or conversely, magnetization is induced under the application of an external electric field [1–3]. To date, different magnetic sensors based on ME composites have been experimentally and theoretically investigated in order to obtain the best ME coupling through changing the structures [4–7], materials [8–10], number of layers [11,12], etc.

Among the proposed composites, the 2-2 laminated composite material has a good ME coupling effect at room temperature, a large degree of freedom in design, and a strong application prospect, which provides a clear physical meaning for the design of a new generation of electronic devices [1–12]. Recently, for static or quasi-static magnetic field sensing in an unshielded room temperature and pressure and lab environment, a high direct current (DC) magnetic field sensitivity of 2.8 Hz/nT and a limit of detection of 800 pT were reported in the NEMS AlN/FeGaB resonator [13]. For alternating current (AC) magnetic field sensing, an extremely low equivalent magnetic noise of 5.1 pT/$\sqrt{\text{Hz}}$ at 1 Hz was reported in the Metglas/piezofiber structure [14]. A super-high magnetic sensitivity of 1.35×10^{-13} T was directly detected at 23.23 kHz in the 1D (1-1) connectivity ME composites of Metglas/PMN-PT [15].

In practice, transient pulsed magnetic field measurement exists in many fields, such as lightning current in power systems [16,17] and aircrafts [18,19], crack detection with pulsed magnetic flux leakage techniques [20,21], and transient electromagnetic measurement in transformer substations [22]. However, to date, most of the reported theoretical and experimental studies carried out on ME sensors have been investigated under the premise of static magnetic field and standard sine wave magnetic field excitation [1–15]. Only a few studies have focused on the transient response of ME materials in pulsed magnetic fields [23]. The magnetic–mechanical–electric nonlinear coupling mechanism of the magnetostrictive/piezoelectric structure should be different by changing the parameters of transient magnetic fields. Thus, for potential applications in pulsed magnetic field measurement of the ME composite, this paper focused on the transient nonlinear ME response under a pulsed magnetic field. The influence of the pulsed magnetic field parameters and external bias field on the ME structure were investigated in detail.

2. Experimental

The ME structure consists of $Fe_{73.5}Cu_1Nb_3Si_{13.5}B_9$ (FeCuNbSiB) and piezofiber, as shown in Figure 1a,b. The FeCuNbSiB (International standard trademark 1K107, produced by Foshan Huaxin Microlite Metal Co., Ltd., Foshan, China) is a pizeomagnetic phase with a high permeability (μr = 30,000), high saturation magnetization ($\mu_0 Ms$ = 1.45 T), and a large anisotropic constant (−30,000 J/m^3). The dimensions of the FeCuNbSiB foils are 10 × 6 × 0.025 mm^3. The Pb(Zr, Ti)O_3 fiber composite (piezofiber) (M4010-P1, provided by Smart Material Cor., Sarasota, FL, U.S.A.) is a piezoelectric phase consisting of rectangular piezoceramic rods (40 mm long and 180 μm thick) sandwiched between layers of adhesive, electrodes, and polyimide film. The electrodes are attached to the film in an interdigitated pattern which transfers the applied voltage directly to and from the ribbon-shaped rods.

As shown in Figure 1a, two FeCuNbSiB layers (each made by three FeCuNbSiB foils) were subsequently laminated to both the top and bottom surfaces of the Pb(Zr, Ti)O_3 (PZT)-fiber layer. Under an AC magnetic field, a mechanical strain was generated in the FeCuNbSiB layer and was then transferred to the piezofiber, resulting in the generation of charges due to the direct piezoelectric effect. As shown in Figure 1b, the ME FeCuNbSiB/piezofiber was designed to operate as a half-wavelength longitudinal resonator vibrating freely at both ends. Thus, one mechanical anchor (made by Beryllium bronze plate, produced by Shanghai Dayu Metal Products Co., Ltd., Shanghai, China) bonded with epoxy at the middle of the FeCuNbSiB/piezofiber where the displacement was zero.

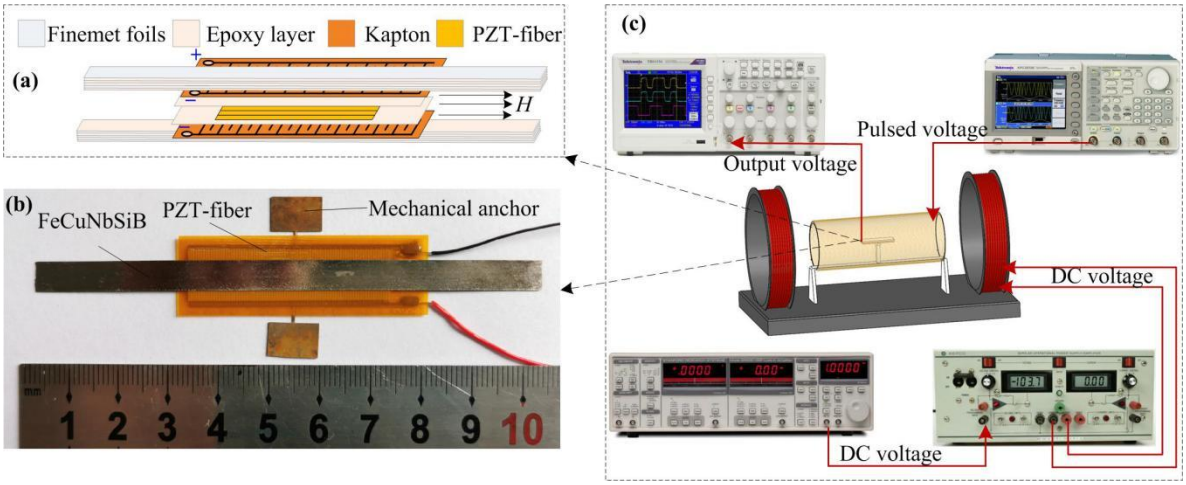

Figure 1. (**a**) Schematic illustrations of the FeCuNbSiB/piezofiber magnetoelectric (ME) composites, (**b**) photograph of the FeCuNbSiB/piezofiber ME composites, (**c**) schematic illustrations of the experimental setup.

The experimental setup is shown in Figure 1c. A signal generator (Tektronix AFG3021B, Tektronix Inc., Beaverton, OR, USA) provided a controllable input current to a long straight solenoid coil with 1800 turns and a 182 mm length, which was used to provide the pulsed magnetic field. A Helmholtz coil (Linkphysics Co., Ltd., Shanghai, China) was used to provide the DC bias magnetic field, which was driven by a power amplifier (KEPCO Bipolar Operational Power Supply, KEPCO Inc., Flushing, NY, USA.). The ME output voltages of the FeCuNbSiB/piezofiber laminate were measured with a lock-in amplifier (SR-830, SRS, Sunnyvale, CA, USA.) and an oscilloscope (Tektronix Inc., Beaverton, OR, USA). The bias magnetic field H_{bias} was measured with a Gauss meter. The AC magnetic field was calculated in the experiments. The resistance of the long straight solenoid coil was measured as 37.8 Ω by a multimeter (Fluke Corporation, Everett, WA, USA). In addition, the voltage of the long straight solenoid in the experiments was measured by an oscilloscope. Thus, the actual current *I* in the long straight solenoid can be calculated as I = voltage/37.8. Then, the AC magnetic field of the central solenoid H = n*I (A/m), where n = 1800/0.182. Before the experiments, the calculated AC magnetic field was calibrated by a Fluxgate probe (CH-Magnetoelectricity Technology, Beijing, China).

3. Results and Discussion

The ME response of the FeCuNbSiB/piezofiber composite was calibration-tested under a standard sine magnetic field. Figure 2a shows the ME coefficient α_{ME} and the phase angle as a function of the bias magnetic field H_{bias} driven at a 1 kHz sine magnetic field. As shown in Figure 2a, α_{ME} increased with increasing H_{bias} up to about H_{bias} = 3.6 Oe reached a maximum value of α_{ME} = 9.2 mV/Oe and then gradually decreased as H_{bias} was further increased. The induced voltage was independent of H_{bias} history and no offset value was found near H_{bias} = 0 Oe. These characteristics are quite important to magnetic field detection. In addition, as the direction of H_{bias} was changed, a 180° phase shift was found, as shown in Figure 2a. Next, α_{ME} was measured as a function of the AC magnetic field frequency at H_{bias} = 5.2 Oe while sweeping near the mechanical resonance, as shown in Figure 2b. As this figure shows, the fundamental resonant frequency for the FeCuNbSiB/piezofiber composite was ~26.47 kHz. At this resonant frequency, a value of α_{ME} > 50 mV/Oe was reached. The natural period of the FeCuNbSiB/piezofiber composite $T = 1/f_r$ = ~37.78 μs.

For the ME composite consisting of mechanically coupled magnetostrictive and piezoelectric layers, the resonance frequency of the ME composite is [12]

$$f_r = \frac{1}{2l}\sqrt{\frac{1}{\rho s}} \quad (1)$$

where l is the length, and ρ and s are the average density and the equivalent elastic compliance, respectively. The length of the PZT-fiber is 40 mm. The ρ_p and s_{11}^E of PZT-fiber is 5.44 g/cm^3 and 32.96×10^{-12} m^2/N, respectively. The length of the FeCuNbSiB foils is 100 mm. The ρ_m and $s_{33,m}^H$ of FeCuNbSiB is 7.25 g/cm^3 and 5.2×10^{-12} m^2/N, respectively. The calculated first-order longitudinal resonant frequencies of the PZT-fiber and the FeCuNbSiB foil are ~29.5 kHz and ~25.8 kHz, respectively. Thus, the resonant frequency for the FeCuNbSiB/PZT-fiber stack should be about ~25.8 kHz to ~29.5 kHz. In order to calculate the resonance frequency of FeCuNbSiB/piezofiber, we used the ANSYS 19.0 software (ANSYS, Inc., Canonsburg, PA, USA). In the simulations, the elastic modulus and density of the epoxy layer were 3 GPa and 5 g/cm^3, respectively. The simulation results of the first-order longitudinal vibration are shown in the inset of Figure 2b. The first-order longitudinal resonant frequency of the FeCuNbSiB/PZT-fiber was ~28.14 kHz. The theory calculated and the simulation results agree with the experimental results.

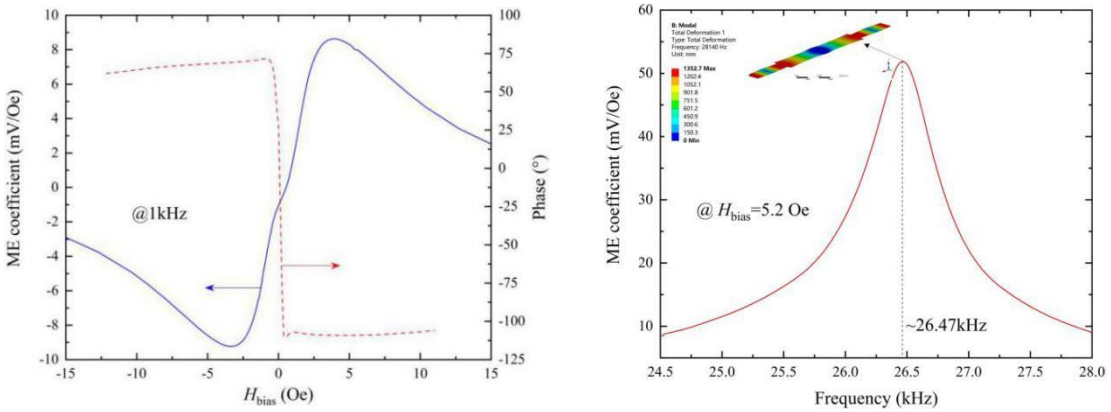

(**a**) (**b**)

Figure 2. The ME voltage coefficient of the FeCuNbSiB/piezofiber laminates: (**a**) ME coefficient α_{ME} as a function of the bias magnetic field H_{bias} in response to a ~1 kHz sine driving magnetic field, and (**b**) α_{ME} as a function of the AC sine magnetic drive frequency sweeping through the electromechanical resonance.

Then, the transient nonlinear ME coupling was investigated in detail. Figure 3 shows the time dependence output voltage V_o of the FeCuNbSiB/piezofiber structure driven by the magnetic field pulse with a width (Δt) of ~100 μs and an amplitude of 51 Oe. The inset of Figure 3 shows the detail when times were 0–200 μs. The rise time of the pulse magnetic was ~8.4 ns. From this figure, the V_o increased gradually when the pulsed magnetic field increased rapidly to an amplitude of 51 Oe and maintained ~100 μs. This is because the magnetic energy increased gradually when the pulsed field maintained the amplitude. It is clear that V_o oscillated at the period Δt_1 = ~37.78 μs. After t > Δt = 100 μs, the pulse magnetic field decreased rapidly to zero. However, the V_o decreased gradually and oscillated at the period Δt_2 = ~37.78 μs. This is due to the inertia effect of the FeCuNbSiB/piezofiber structure. The FeCuNbSiB/piezofiber ME structure is a mechanical resonant structure that self-vibrates near the equilibrium position at the natural period T when the pulsed magnetic field vanishes. It is clear that the FeCuNbSiB/piezofiber structure always oscillates at the natural period T in the time domain. If the width of the pulsed magnetic field Δt is equal to T or multiples of T, what will happen?

Figure 4 shows the time dependence V_o of the FeCuNbSiB/piezofiber structure driven by magnetic field pulses with amplitudes of 51 Oe and widths of Δt = T–5T. The inset of Figure 4 shows the detail when times were 0–250 μs. After t >Δt, it is interesting that the self-vibration phenomena vanished when Δt = T–5T, which is extremely different from Figure 3. This result can be explained by the fact that the FeCuNbSiB/piezofiber structure was exactly in an equilibrium position when the pulse magnetic field vanished. Moreover, the other interesting result from Figure 4 is that V_o grew exponentially, which was excited by the same amplitude pulsed magnetic field of 51 Oe when Δt = T–5T. This result demonstrates that the ME FeCuNbSiB/piezofiber structure can be used as a pulse magnetic width measured device, and this will be investigated in detail in the following section.

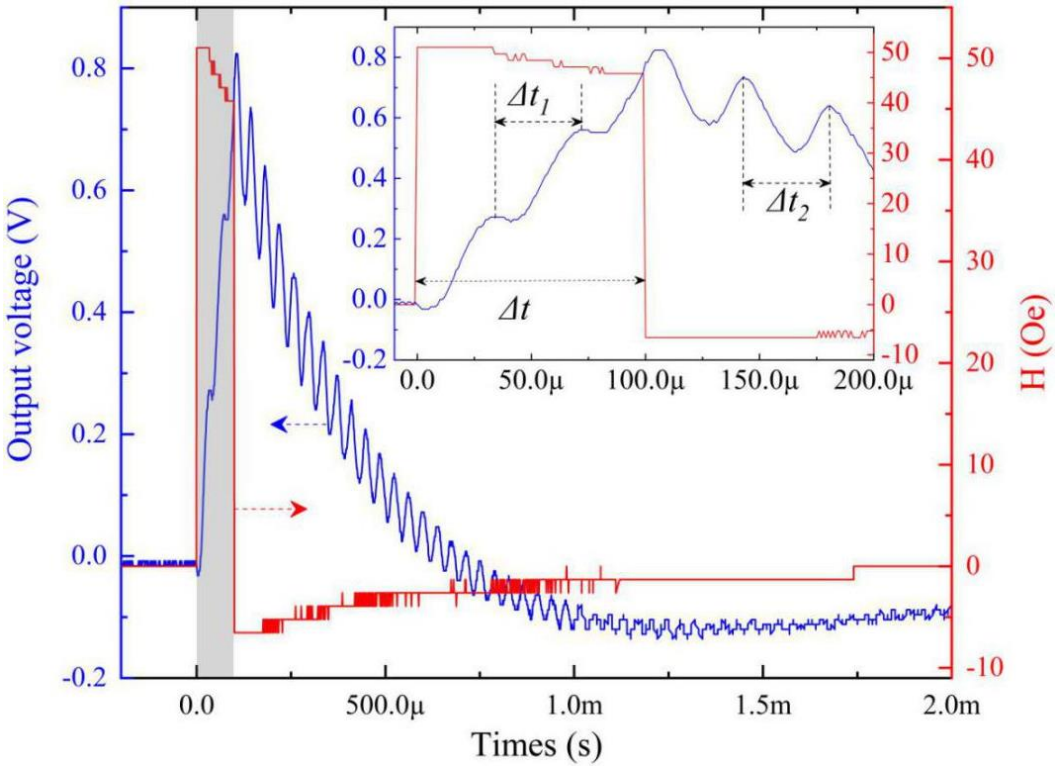

Figure 3. Time dependence output voltage V_o of the FeCuNbSiB/piezofiber structure driven by the magnetic field pulse with a width (Δt) of ~100 μs and an amplitude of 51 Oe. The inset shows the detail when times were 0–200 μs. The rise time of the pulse magnetic was ~8.4 ns. The bias magnetic field was set to zero.

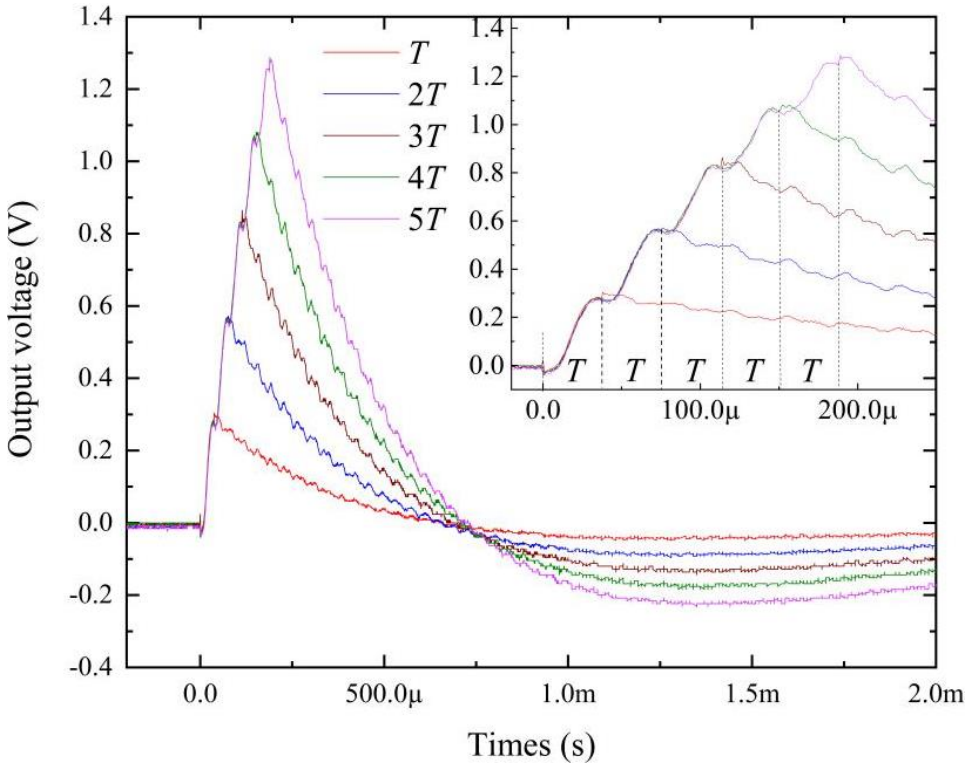

Figure 4. Time dependence output voltage V_o of the FeCuNbSiB/piezofiber structure driven by the magnetic field pulse with an amplitude of 51 Oe and a width of Δt = T–5T. The rise time of the pulse magnetic was ~8.4 ns. The bias magnetic field was set to zero.

Based on Figure 2a, the ME response of the FeCuNbSiB/piezofiber structure is dependent on the H_{bias}. Therefore, the H_{bias} dependence of the ME response for the FeCuNbSiB/piezofiber structure driven by the pulsed magnetic field was also investigated. Figure 5 shows the peak output voltage V_p (maximum V_o in Figure 3) as a function of H_{bias} for the FeCuNbSiB/piezofiber structure driven by the pulsed magnetic field with Δt = ~100 μs. The curve tendency in this figure is the same as that in Figure 2a. The maximum V_p was ~0.9 V at H_{bias} = 3.6 Oe.

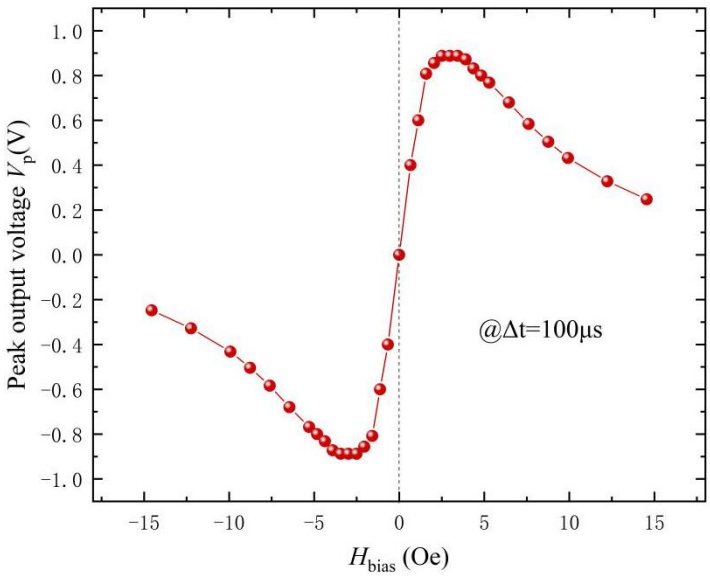

Figure 5. The peak output voltage V_p (maximum V_o in Figure 3) as a function of H_{bias} for the FeCuNbSiB/piezofiber structure driven by the pulsed magnetic field with Δt = ~100 μs.

Next, the transient sensing characteristics of the FeCuNbSiB/piezofiber structure was investigated. Firstly, the amplitude of the pulsed magnetic field H_A sensitivity was measured. Consequently, Figure 6 shows the peak output voltage (like the peak in Figure 3) as a function of H_A at H_{bias} = 0 Oe. The different values of amplitude of the pulsed magnetic field H_A were obtained at Δt = ~100 μs. The linear fitting expression based on the experimental data was $V_p = 0.017H_A - 0.0433$. Based on Figure 6, it is obvious that the induced ME voltage had a near linear (R^2 = 0.9675) relation with H_A. The observation indicates an improved detection sensitivity of 17 mV/Oe. Clearly, the presented FeCuNbSiB/piezofiber sensor seems to be an ideal application for the detection of amplitude variations of pulsed magnetic fields.

From Figure 4, changing Δt results in the variation of the output voltage of the FeCuNbSiB/piezofiber structure. Figure 7 shows the peak output voltage (like the peak in Figure 3) as a function of the width of the pulsed magnetic field Δt = 0–500 μs as H_{bias} = 0 Oe. It is evident that the V_p increases with Δt and reaches its maximum value after Δt >300 μs. For the linear fitting at Δt = 0–300 μs, the relationship between V_p and Δt is $V_p = 0.0054\Delta t + 0.212$. One can see that the linear (R^2 = 0.9757) dependence of the V_p on the Δt takes place in a region of $0 < \Delta t < 300$ μs. Based on the slope of the plots, the sensitivity of the FeCuNbSiB/piezofiber structure for pulsed width sensing was determined to be 5.4 mV/μs. It can be concluded that this ME sensor is suitable for pulsed width measurement fields, such as lightning current monitoring.

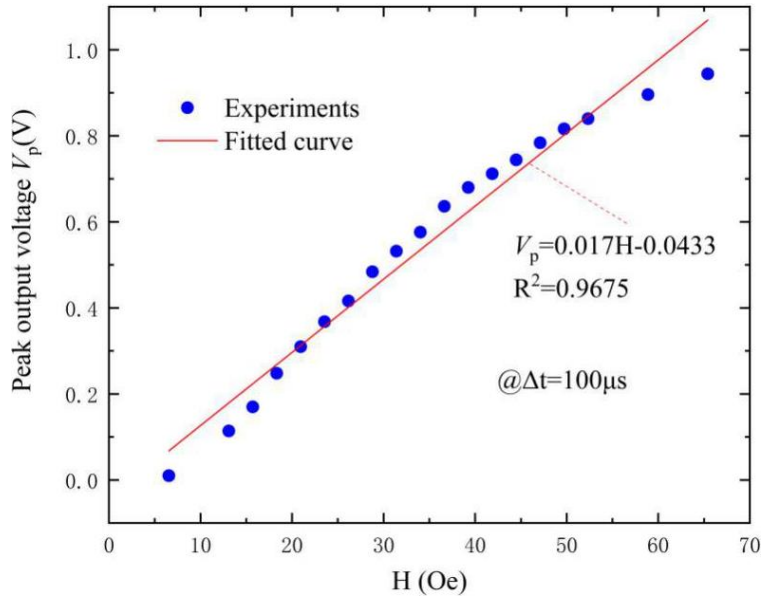

Figure 6. The peak output voltage V_p (maximum V_o in Figure 3) as a function of the amplitude of the pulsed magnetic field H_A for the FeCuNbSiB/piezofiber structure driven by the pulsed magnetic field with Δt = ~100 μs. The red line is the linear approximation.

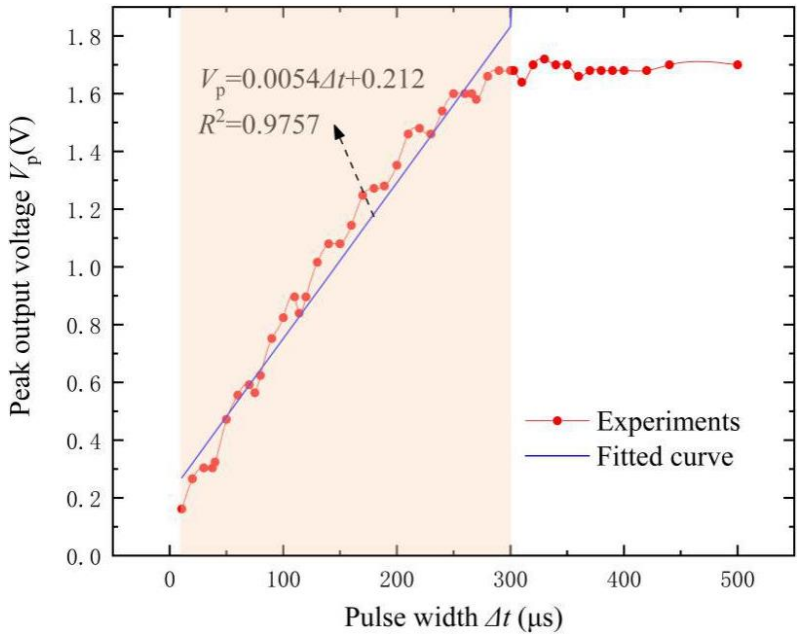

Figure 7. The peak output voltage V_p (maximum V_o in Figure 3) as a function of the width of the pulsed magnetic field Δt for the FeCuNbSiB/piezofiber structure at H_{bias} = 0 Oe. The blue line is the linear approximation. The amplitude of the pulsed magnetic field is 52.3 Oe.

4. Conclusions

In conclusion, a FeCuNbSiB/piezofiber structure prototype was fabricated and several experiments were conducted to illuminate the transient nonlinear ME response. The time dependence output voltage of the FeCuNbSiB/piezofiber structure was measured in the experiments, which showed that the FeCuNbSiB/piezofiber structure oscillated during the natural period T = ~37.78 μs in the time domain. Specifically, the self-vibration phenomena vanished after the excited field vanished when the width was equal to the multiples of the natural period T. The transient ME response was strongly dependent on the external bias magnetic field, which was the same as with the ME response driven by

the sine magnetic field. The sensing characteristics to the pulsed magnetic field were also measured. The results show that the output sensitivities reached 17 mV/Oe Δt = 100 μs for detecting the amplitude of the pulse magnetic field and reached 5.4 mV/μs when Δt = 0–300 μs for detecting the pulsed width. The results obtained may be useful for the development of ME sensors for pulsed magnetic fields, such as the lighting current monitoring field.

Author Contributions: C.L. designed the project; H.Z. developed ME composite and carried out experimental works, A.Y. designed the experimental system. Z.O. carried out simulation work. F.Y. performed the experimental works. H.G. performed experiments and analyzed results; C.L. and H.Z. wrote the manuscript.

Funding: This work was supported by the National Natural Science Foundation of China (Grant Nos. 61801402, 51775452), Fundamental Research Funds for the Central Universities (2682019CX35, 2018GF02), and the Science and Technology Program of State Grid Jiangxi Electric Power Co., Ltd. (No. 521820180004).

Conflicts of Interest: The authors declare no conflict of interest.

References

1. Lawes, G.; Srinivasan, G. Introduction to magnetoelectric coupling and multiferroic films. *J. Phys. D Appl. Phys.* **2011**, *44*, 243001. [CrossRef]
2. Vaz, C.A.F.; Hoffman, J.; Ahn, C.H.; Ramesh, R. Magnetoelectric Coupling Effects in Multiferroic Complex Oxide Composite Structures. *Adv. Mater.* **2010**, *22*, 2900–2918. [CrossRef]
3. Chu, Z.; PourhosseiniAsl, M.; Dong, S. Review of multi-layered magnetoelectric composite materials and devices applications. *J. Phys. D Appl. Phys.* **2018**, *51*, 243001. [CrossRef]
4. Lu, C.; Li, P.; Wen, Y.; Yang, A. Large Self-Biased Magnetoelectric Properties in Heterostructure of Graded-Magnetostrictive Layers and a Rosen-Type Piezoelectric Transformer. *IEEE Sens. J.* **2015**, *15*, 402–407. [CrossRef]
5. Salzer, S.; Jahns, R.; Piorra, A.; Teliban, I.; Reermann, J.; Höft, M.; Quandt, E.; Knöchel, R. Tuning fork for noise suppression in magnetoelectric sensors. *Sens. Actuators A* **2016**, *237*, 91–95. [CrossRef]
6. Li, P.; Wen, Y.; Huang, X.; Yang, J.; Wen, J.; Qiu, J.; Zhu, Y.; Yu, M. Wide-bandwidth high-sensitivity magnetoelectric effect of magnetostrictive/piezoelectric composites under adjustable bias voltage. *Sens. Actuators A* **2013**, *201*, 164–171. [CrossRef]
7. Rupp, T.; Truong, B.D.; Williams, S.; Roundy, S. Magnetoelectric Transducer Designs for Use as Wireless Power Receivers in Wearable and Implantable Applications. *Materials* **2019**, *12*, 512. [CrossRef]
8. Zhang, J.; Kang, Y.; Gao, Y.; Weng, G.J. Experimental Investigation of the Magnetoelectric Effect in NdFeB-Driven A-Line Shape Terfenol-D/PZT-5A Structures. *Materials* **2019**, *12*, 1055. [CrossRef]
9. Zhang, R.; Zhang, S.; Xu, Y.; Zhou, L.; Liu, F.; Xu, X. Modeling of a Magnetoelectric Laminate Ring Using Generalized Hamilton's Principle. *Materials* **2019**, *12*, 1442. [CrossRef]
10. Ou, Z.; Lu, C.; Yang, A.; Zhou, H.; Cao, Z.; Zhu, R.; Gao, H. Self-biased magnetoelectric current sensor based on $SrFe_{12}O_{19}$/FeCuNbSiB/PZT composite. *Sens. Actuators A* **2019**, *290*, 8–13. [CrossRef]
11. Wang, Y.; Gray, D.; Berry, D.; Li, M.; Gao, J.; Li, J.; Viehland, D. Influence of interfacial bonding condition on magnetoelectric properties in piezofiber/Metglas heterostructures. *J. Alloys Compd.* **2012**, *513*, 242–244. [CrossRef]
12. Tang, C.; Lu, C. Strong self-biased magnetoelectric charge coupling in a homogenous laminate stack for magnetic sensor. *J. Alloys Compd.* **2016**, *686*, 723–726. [CrossRef]
13. Li, M.; Matyushov, A.; Dong, C.; Chen, H.; Lin, H.; Nan, T.; Qian, Z.; Rinaldi, M.; Lin, Y.; Sun, N.X. Ultra-sensitive NEMS magnetoelectric sensor for picotesla DC magnetic field detection. *Appl. Phys. Lett.* **2017**, *110*, 143510. [CrossRef]
14. Wang, Y.; Gray, D.; Berry, D.; Gao, J.; Li, M.; Li, J.; Viehland, D. An Extremely Low Equivalent Magnetic Noise Magnetoelectric Sensor. *Adv. Mater.* **2011**, *23*, 4111–4114. [CrossRef]
15. Chu, Z.; Shi, H.; Shi, W.; Liu, G.; Wu, J.; Yang, J.; Dong, S. Enhanced Resonance Magnetoelectric Coupling in (1-1) Connectivity Composites. *Adv. Mater.* **2017**, *29*, 1606022. [CrossRef]
16. Kawabata, T.; Yanagawa, S.; Takahashi, H.; Yamamoto, K. Development of a shunt lightning current measuring system using a Rogowski coil. *Electr. Power Syst. Res.* **2015**, *118*, 110–113. [CrossRef]

17. Mei, H.; Yan, S.; Zhao, C.; Wang, L. Research on Lightning Current Sensor Coil Based on Lightning Space Magnetic Field. *IEEE Trans. Intrum. Meas.* **2018**, *67*, 1922–1928. [CrossRef]
18. Van Deursen, A.P.J.; Stelmashuk, V. Inductive Sensor for Lightning Current Measurement, Fitted in Aircraft Windows—Part I: Analysis for a Circular Window. *IEEE Sens. J.* **2011**, *11*, 199–204. [CrossRef]
19. Van Deursen, A.P.J. Inductive sensor for lightning current measurement, fitted in aircraft windows—Part II: Measurements on an a320 aircraft. *IEEE Sens. J.* **2011**, *11*, 205–209. [CrossRef]
20. Zhou, D.; Pan, M.; He, Y.; Du, B. Stress detection and measurement in ferromagnetic metals using pulse electromagnetic method with U-shaped sensor. *Measurement* **2017**, *105*, 136–145. [CrossRef]
21. Sophian, A.; Tian, G.Y.; Zairi, S. Pulsed magnetic flux leakage techniques for crack detection and characterization. *Sens. Actuators A* **2006**, *125*, 186–191. [CrossRef]
22. Wang, L.; Huang, J.; Ji, J.; Pang, F.; Yuan, Y. Measurement of transient electromagnetic coupling and interference caused by disconnector operation in substation. *Measurement* **2017**, *96*, 1–7.
23. Kreitmeier, F.; Chashin, D.V.; Fetisov, Y.K.; Fetisov, L.Y.; Schulz, I.; Monkman, G.J.; Shamonin, M. Nonlinear Magnetoelectric Response of Planar Ferromagnetic-Piezoelectric Structures to Sub-Millisecond Magnetic Pulses. *Sensors* **2012**, *12*, 14821–14837. [CrossRef]